

PERFORMANCE OF FRONT VELOCITY ON SLOPE IN A 1D RAPID DEBRIS FLOW NUMERICAL MODEL

VAN KHOI PHAM*, THI-HONG-NGOC DOAN

Faculty of Civil Engineering, Vietnam Maritime University, Vietnam

*Corresponding author: khoipv.ctt@vimaru.edu.vn

DOI: <https://doi.org/10.65154/jmst.2025.i84.822>

Abstract

Landslides and debris flows are among the most destructive natural hazards, posing serious threats to human life, infrastructure, and socio-economic development. Rapid debris flows occurring on steep slopes are particularly dangerous due to their high mobility and destructive front velocity. Accurate prediction of the front velocity, the leading edge speed of the moving mass, is critical for hazard assessment, runout estimation, and engineering countermeasures. This study develops and evaluates the one-dimensional (1D) numerical model to investigate the performance of front velocity on slopes for rapid debris flows governed by Coulomb-type rheology. The governing equations are derived from depth-averaged nonlinear shallow water formulations, modified to account for slope gradients and internal frictions. The model applies a hybrid finite difference-finite volume scheme for spatial discretization, ensuring numerical stability and accuracy in capturing steep slope dynamics. Numerical experiments are conducted across a range of slope angles and rheological parameters, which generate 16 scenarios, to analyze their effects on debris front velocity values. Results indicate that the front velocity is highly sensitive to small bottom slope angles under different internal friction angles. A linear relationship between debris front velocities and bottom slope angles, as well as a nonlinear relationship between simulation times, debris lengths and bottom slope angles are identified in this study. For future research, more rheological models should be incorporated into the resistance terms, and the approach should be extended to two-dimensional models.

Keywords: Front velocity, rapid debris flow, numerical model, nonlinear shallow water equations, slope.

1. Introduction

Debris flows, or landslides, are among the most destructive natural hazards, causing severe damage to infrastructure and posing significant risks to human life and livelihoods worldwide [1-6]. In tropical and mountainous regions, prolonged rainfall, earthquakes, and rapid snowmelt often trigger large-scale slope failures that mobilize enormous masses of soil and rock. Historical events, such as the 2008 Wenchuan earthquake-induced landslides in China [3] and the 2011 Umyeon landslide in South Korea [4-5], highlight the devastating consequences of these disasters, which include loss of life, destruction of transportation networks, and long-term disruption of local communities. Due to the increasing frequency and intensity of extreme weather events under climate change, understanding and predicting landslide behavior has become an urgent task for disaster risk reduction and infrastructure safety [7, 8].

To improve hazard prediction and mitigation, numerical modeling of landslides and debris flows has emerged as an indispensable tool. Numerical simulations enable researchers to replicate initiation, propagation, and deposition processes that are difficult or dangerous to measure in the field [5], [6], [8]. Various approaches have been proposed, ranging from depth-averaged shallow water-type equations to discrete element methods. These models provide insights into flow dynamics such as velocity distribution, runout distance, and impact forces on structures. Despite these advances, challenges remain in capturing the rapid and highly nonlinear nature of debris flow motion, especially when the flow involves steep slopes and heterogeneous materials [9, 10].

Among the different types of mass movement, rapid debris flows governed by Coulomb-type rheology are of particular interest [1], [11]. These flows occur on steep mountain slopes, where loose material accelerates rapidly under gravity, often reaching destructive front velocity. The front velocity, which is defined as the leading edge speed of the moving mass, plays a critical role in determining the runout length, impact pressure, and potential damage

to downstream areas. Accurate prediction of front velocity in 1D numerical models is therefore essential for risk assessment and engineering countermeasures.

The present study addresses this gap by investigating the performance of front velocity on slopes within a 1D rapid debris flow numerical model, with emphasis on the Coulomb-type behavior of landslide motion. By analyzing the relationship between slope gradient, rheological parameters, and flow front propagation, this research provides valuable insights for improving debris flow hazard modeling and informing practical disaster mitigation strategies.

2. Debris flow numerical model

2.1. Governing equations and rapid model

In this study, we investigate a 1D debris flow numerical model on a slope, with variables defined as illustrated in Fig. 1 below [9].

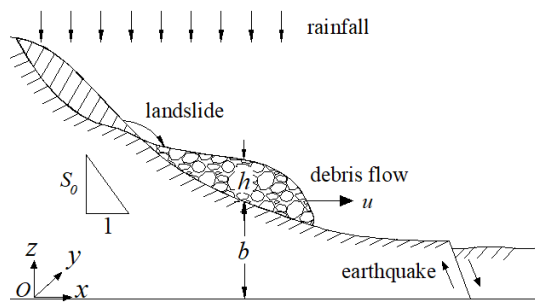


Figure 1. Schematic of debris flow model

The continuity and momentum equations derived from the nonlinear shallow water equations are given as:

$$\frac{\partial h}{\partial t} + \frac{\partial(hu)}{\partial x} = 0 \quad (1)$$

$$\frac{\partial(hu)}{\partial t} + \frac{\partial(hu^2)}{\partial x} + \frac{1}{2}g \frac{\partial h^2}{\partial x} = gh(S_0 - S_f) \quad (2)$$

Where h is the debris flow depth, u is the particle debris flow velocity in the x -direction, g is the gravitational acceleration, S_0 ($= \tan \theta = -\partial b / \partial x$) is the bottom slope source term, θ is the bottom slope angle, b is the bottom of the non-erodible bed, and S_f is the resistance source term.

In the source term of momentum equation (2), S_0 is assumed to be positive and depends on the initial condition of slope angle, S_f is determined by resistance terms as follows [1], [7], [12]:

$$S_f = \cos \theta \tan \varphi + \frac{n^2 u |u|}{h^{4/3}} + \frac{\tau_y}{\rho g h} \quad (3)$$

Where the first term represents Coulomb resistance, which accounts for the internal friction of the debris material (φ). The second term denotes turbulent resistance, describing the surface friction between debris and the non-erodible bed (i.e., the Manning coefficient n). The last term corresponds to yield resistance, which reflects the inherent yield strength of the debris material (τ_y). And, ρ is the debris density. When all three resistance terms are considered, the debris flow is significantly slowed. Conversely, if some resistance terms are neglected, the flow becomes more rapid. In this study, the latter two terms (i.e., roughness coefficient and yield strength) are neglected due to the idealized initial conditions of the numerical domain [9], [11]. The resulting formulation thus becomes a rapid debris flow model governed solely by Coulomb resistance, as expressed below:

$$S_f = \cos \theta \tan \varphi \quad (4)$$

2.2. Numerical scheme and model verification

The governing equations (1) and (2) can be written in conservative form as follows:

$$\frac{\partial U}{\partial t} + \frac{\partial F(U)}{\partial x} = H(U) \quad (5)$$

Where:

$$U = \begin{pmatrix} h \\ hu \end{pmatrix} \quad (6)$$

$$F(U) = \begin{pmatrix} hu \\ hu^2 + \frac{1}{2}gh^2 \end{pmatrix} \quad (7)$$

$$H(U) = \begin{pmatrix} 0 \\ gh(S_0 - S_f) \end{pmatrix} \quad (8)$$

And U is the vector of conserved variables; $F(U)$ and $H(U)$ are the flux term and source term, respectively. Equation (5) is solved using the hybrid finite volume-finite difference method for spatial integration and the implicit method for time integration [13], [15]. This numerical model was successfully verified against the Dressler analytical solution for debris flow over a steep slope of 45° as presented in [9]. In the present study, we focus on investigating the fast front velocity of rapid debris flow under real disaster conditions. Therefore, the

verification process is not repeated here.

3. Numerical simulations of rapid debris flow model on slopes

In this section, we simulate debris flow on slopes using the Coulomb resistance as the 1D rapid landslide model to describe the flow characteristics. The slope angle of 45° , the internal friction angle of 5° , and the unit debris volume of 1m^3 at the unit width of numerical flume ($w_f=1\text{m}$) are set as the initial conditions (see Fig. 2). The chosen initial unit debris volume of $V = 1\text{m}^3$ is representative of other volumes, which can be easily determined by rational scaling. In all numerical domains in this study, a grid size of 1 cm and a Courant number of 0.9 are adopted to ensure numerical stability.

In Fig. 2, the source point O is defined at the front of the initial debris volume, the initial depth is set as $h_i=1.41\text{m}$, the initial length of the debris body is $l_i=1.41\text{m}$, and the release height is $H=20\text{m}$. This initial height H is selected to ensure that the debris mass continues to move downslope until the entire volume passes over the source point O . At that point, l represents the dynamic length of the debris flow body along the slope.

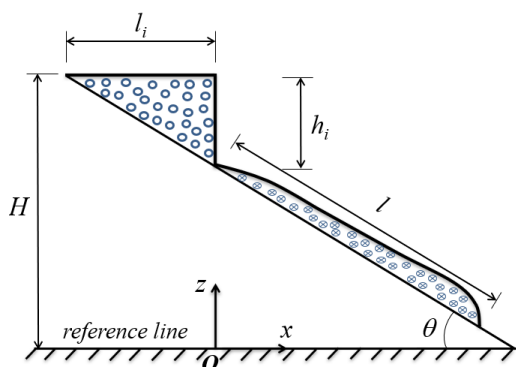
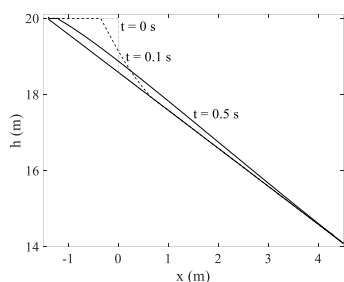
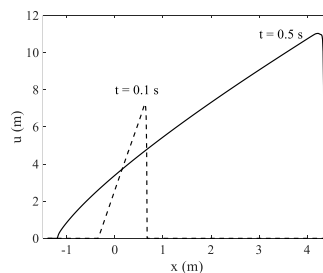


Figure 2. Debris flow simulation on slope

Fig. 3 presents the simulated flow depths and velocities across the entire computational domain at



a) Debris flow depth



b) Debris flow velocity

Figure 3. Debris flow heights and velocities at different times

$t=0.1\text{s}$ and $t=0.5\text{s}$.

In Fig. 3a, at $t=0.1\text{s}$, the debris depth increases on the right side and decreases on the left side of the source point O . As time progresses, at $t=0.5\text{s}$, the debris flow moves downslope to the right, forming a thinner depth but extending over a longer distance, in contrast to the left side. In Fig. 3b, at $t=0.1\text{s}$, the debris velocity increases from the tail (left side) to the front (right side), reaching its maximum at the flow front. At $t=0.5\text{s}$, the velocity profile follows a similar pattern but exhibits a higher front velocity. At each time step, the horizontal displacement of the front is determined, and the debris flow length is calculated through the slope angle θ . The simulation terminates once the entire initial debris volume has moved downslope past the source point O . In that moment, the initial potential energy of the debris mass is fully transformed into kinetic energy. From these results, we determine the debris front velocity (u_f), the debris time-consuming (t_f), and the debris length (l_f).

4. Performance of debris front velocity on slopes

The debris flow simulation is carried out for different bottom slope angles and internal friction angles to investigate the variation of debris front velocity. In this study, we consider three additional internal friction angles of 0° , 10° , and 15° , together with three additional slope angles of 40° , 35° , and 30° . These conditions, combined with the base case, result in a total of 16 simulation scenarios, as summarized in Table 2. These assumed initial conditions have been employed in various debris flow numerical models to simulate real landslide problems [1-4], [14].

In Table 2, the initial debris length (l_i) and debris depth (h_i) are derived from the unit debris volume $V=1\text{m}^3$, with a unit flume width of $w_f=1\text{m}$, and are computed based on the corresponding slope angle θ for each case.

Table 2. Scenarios for simulations of debris front velocity on slopes with different internal friction angles

$\theta(^{\circ})$	$\varphi(^{\circ})$	$V = 1 \text{ (m}^3\text{)}$	
		$l_i \text{ (m)}$	$h_i \text{ (m)}$
30	0; 5; 10; 15	1.86	1.08
35	0; 5; 10; 15	1.69	1.18
40	0; 5; 10; 15	1.54	1.30
45	0; 5; 10; 15	1.41	1.41

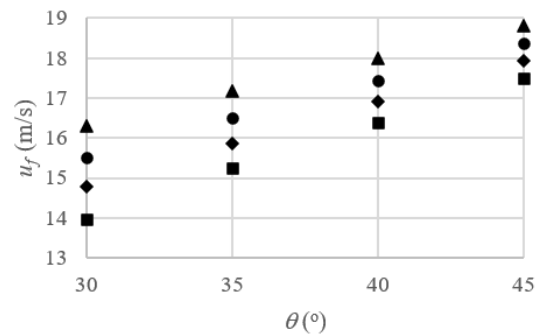
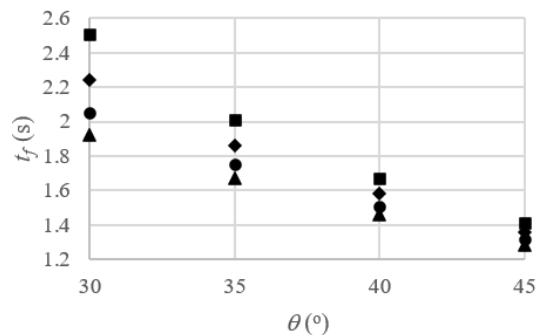
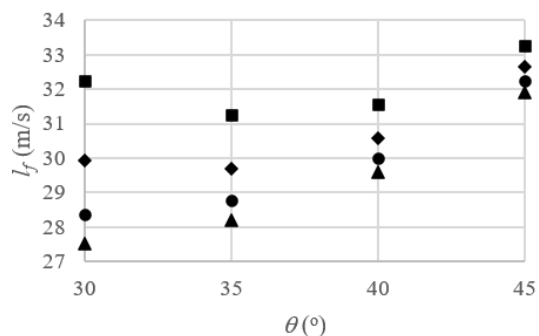
Table 3. Debris characteristics on slopes

$\theta(^{\circ})$	$\varphi(^{\circ})$	$u_f \text{ (m/s)}$	$t_f \text{ (s)}$	$l_f \text{ (m)}$
30	0	16.29	1.92	27.53
	5	15.52	2.05	28.38
	10	14.77	2.24	29.92
	15	13.97	2.51	32.25
35	0	17.17	1.67	28.20
	5	16.51	1.75	28.76
	10	15.87	1.86	29.69
	15	15.24	2.01	31.25
40	0	17.99	1.46	29.58
	5	17.45	1.51	30.00
	10	16.9	1.58	30.59
	15	16.38	1.67	31.58
45	0	18.82	1.28	31.90
	5	18.38	1.32	32.24
	10	17.94	1.36	32.65
	15	17.49	1.41	33.28

Table 3 presents the debris front velocity, travel time, and length across 16 simulation scenarios with varying internal friction angles and bottom slope angles.

In Table 3, the maximum front velocity is 18.82m/s ($\sim 68\text{km/h}$), obtained for the case of the steepest slope angle ($\theta=45^{\circ}$) combined with the lowest internal friction angle ($\varphi=0^{\circ}$ represents the water case). Conversely, the minimum front velocity is 13.97m/s ($\sim 50 \text{ km/h}$), corresponding to the mildest slope ($\theta=30^{\circ}$) and the highest internal friction angle ($\varphi=15^{\circ}$). These results are physically reasonable, reflecting the balance between the bed slope source term (S_b) and the resistance source term (S_f) in the momentum equation (2).

Figs. 4, 5, and 6 illustrate the performance of debris front velocity, travel time, and flow length on slopes with varying internal friction angles, respectively.

**Figure 4. Performance of debris front velocity on slopes****Figure 5. Performance of debris travel time on slopes****Figure 6. Performance of debris length on slopes**

Notes: The solid triangle represents for $\varphi=0^{\circ}$; the solid dot represents for $\varphi=5^{\circ}$; the solid diamond represents for $\varphi=10^{\circ}$; the solid square represents for $\varphi=15^{\circ}$.

In Fig. 4, the relationship between front velocity and bottom slope angle is linear: as the slope angle increases, the front velocity also increases. Conversely, when the internal friction angle increases, the front velocity decreases. This behavior is consistent with the increased resistance forces incorporated in the debris flow model. Fig. 5 illustrates a pronounced nonlinear relationship between travel time and slope angle, whereas Fig. 6 highlights a strong nonlinear relationship between debris length and slope angle.

In all three figures, small differences in debris flow characteristics associated with different internal friction angles are observed at larger bottom slope angles, whereas much larger differences are evident at smaller slope angles. This finding can be explained by the balance between the bottom slope source term (S_o) and the resistance source term (S_f) in the momentum equation (2). Table 4 presents the regression coefficients and correlation values for the three relationships discussed above.

Table 4. Regression coefficients and correlation values for relationships of debris front velocity, travel time, and length on slopes with different internal friction angles

Cases	φ	a	b	c	R^2
$u_f \sim \theta$	0	0	0.17	11.26	0.9998
	5	0	0.19	9.83	0.9998
	10	0	0.21	8.47	0.9998
	15	0	0.23	7.00	0.9990
$t_f \sim \theta$	0	0.0007	-	4.14	1
			0.10		
	5	0.0011	-	4.99	1
			0.13		
	10	0.0016	-	6.15	0.9998
			0.18		
$l_f \sim \theta$	15	0.0024	-	7.93	0.9995
			0.25		
	0	0.0165	-	41.12	0.9998
			0.95		
	5	0.0186	-	45.81	0.9999
			1.14		
	10	0.0229	-	55.38	1
			1.54		
	15	0.0270	-	66.65	1
			1.96		

In Table 4, the nonlinear property of the relationships is reflected in the a coefficients, which increase with greater nonlinearity. The positive b coefficients indicate increasing correlations, whereas the negative b coefficients represent decreasing correlations. All correlation coefficients ($R^2 \approx 1$) confirm that the relationships exhibit strong and reliable correlation. Furthermore, interpolation techniques are applied to estimate values at other internal friction angles beyond those directly simulated [16].

5. Conclusion

This paper introduces the performance of front velocity on slope in a 1D rapid debris flow numerical model. The debris front velocity is one of the most important characteristics of debris flows, as it determines the induced forces and informs disaster mitigation strategies. A 1D debris flow model is presented as a rapid numerical model by including only the Coulomb rheology in the resistance term. The governing equations are discretized using a hybrid finite volume-finite difference scheme for spatial integration and an implicit scheme for temporal integration. Numerical simulations of rapid debris flow with a bottom slope angle of 45° and an internal friction angle of 5° at different times are conducted to examine debris front velocity and other characteristics. To evaluate debris front velocity on slopes, 16 scenarios combining slope angles and internal friction angles are established. The results show the values of debris front velocity, travel time, and run out length, which are crucial for disaster prevention. A linear relationship is identified between debris front velocity and slope angle, while nonlinear relationships are observed between simulation times, debris lengths, and slope angle under different internal friction conditions. Future studies should include additional resistance terms in the governing equations and extend to two-dimensional models to more accurately simulate real debris flow processes.

Acknowledgements

This research is funded by Vietnam Maritime University under grant number: **DT25-26.104**.

REFERENCES

- [1] D. Naef, D. Rickenmann, P. Rutschmann, and B. W. McArdeall (2006), *Comparison of flow resistance relations for debris flows using a one-dimensional finite element simulation model*, Nat. Hazards Earth Syst. Sci., Vol.6, No.1, pp.155-165. doi: 10.5194/nhess-6-155-2006.
- [2] V. Medina, M. Hürlimann, and A. Bateman (2008), *Application of FLATModel, a 2D finite volume code, to debris flows in the northeastern part of the Iberian Peninsula*, Landslides, Vol.5, No.1, pp.127-142. doi: 10.1007/s10346-007-0102-3.
- [3] C. Ouyang, S. He, and C. Tang (2015), *Numerical analysis of dynamics of debris flow over erodible beds in Wenchuan earthquake-induced area*,

- Engineering Geology, Vol.194, pp.62-72.
doi: 10.1016/j.enggeo.2014.07.012.
- [4] S. Jeong, Y. Kim, J. K. Lee, and J. Kim (2015), *The 27 July 2011 debris flows at Umyeonsan, Seoul, Korea*, Landslides, Vol.12, No.4, pp.799-813.
doi: 10.1007/s10346-015-0595-0.
- [5] V. K. Pham, C. Lee, and V. N. Vu (2025), *A novel depth-averaged model of landslide over erodible bed using (b, s) coordinates*, Computers and Geotechnics, Vol.180, p.107105.
doi: 10.1016/j.compgeo.2025.107105.
- [6] V. K. Pham (2025), *Performance of Artificial Bed-Wetting Parameter in a 1D Coulomb-Type Debris Flow Numerical Model*, Engineering, Technology & Applied Science Research, Vol.15, No.3, pp.22612-22620.
doi: 10.48084/etasr.10719.
- [7] S. Yavari-Ramshe and B. Ataie-Ashtiani (2016), *Numerical modeling of subaerial and submarine landslide-generated tsunami waves—recent advances and future challenges*, Landslides, Vol.13, No.6, pp.1325-1368.
doi: 10.1007/s10346-016-0734-2.
- [8] M. G. Trujillo-Vela, A. M. Ramos-Cañón, J. A. Escobar-Vargas, and S. A. Galindo-Torres (2022), *An overview of debris-flow mathematical modelling*, Earth-Science Reviews, Vol.232, p.104135.
doi: 10.1016/j.earscirev.2022.104135.
- [9] Phạm Văn Khôi and Vũ Văn Nghi (2023), *Mô hình số một chiều mô phỏng sạt lở đất trên mái dốc lớn: Lý thuyết và kiểm chuẩn với mô hình giải tích*, Tạp chí Khoa học và Công nghệ Việt Nam, bản B, Vol.65, No.11, pp.42-46.
doi: 10.31276/VJST.65(11).42-46.
- [10] L. Zhao, J. Mao, X. Bai, X. Liu, T. Li, and J. J. R. Williams (2016), *Finite element simulation of impulse wave generated by landslides using a three-phase model and the conservative level set method*, Landslides, Vol.13, No.1, pp.85-96.
doi: 10.1007/s10346-014-0552-3.
- [11] S. B. Savage and K. Hutter (1989), *The motion of a finite mass of granular material down a rough incline*, J. Fluid Mech., Vol.199, pp.177-215.
doi: 10.1017/S0022112089000340.
- [12] Phạm Văn Khôi (2025), *Nghiên cứu ảnh hưởng lưu biến của dòng sạt lở đất ngầm tới đặc trưng sóng thần dùng mô hình số tích hợp*, Tạp chí Khoa học Công nghệ Giao thông vận tải, Vol.14, No.2, pp.27-36.
doi: 10.55228/JTST.14(2).27-36.
- [13] S. Nickovic, G. Pejanovic, V. Djurdjevic, J. Roskar, and M. Vujadinovic (2010), *HYPROM hydrology surface-runoff prognostic model: HYDROLOGY PROGNOSTIC MODEL*, Water Resour. Res., Vol.46, No.11.
doi: 10.1029/2010WR009195.
- [14] J. Paik (2015), *A high resolution finite volume model for 1D debris flow*, Journal of Hydro-environment Research, Vol.9, No.1, pp.145-155.
doi: 10.1016/j.jher.2014.03.001.
- [15] V. K. Pham, C. Lee, and V. N. Vu (2019), *Numerical Simulation of Subaerial and Submarine Landslides Using the Finite Volume Method in the Shallow Water Equations with (b, s) Coordinate*, Journal of Korean Society of Coastal and Ocean Engineers, Vol.31, No.4, pp.229-239.
doi: 10.9765/KSCOE.2019.31.4.229.
- [16] Phạm Văn Khôi (2024), *Xác định chiều rộng đê tường đứng rồng dạng ngáp đáp ứng hiệu quả chiết giảm sóng đơn dùng mô hình số và phương trình hồi quy bậc hai*, Tạp chí Khoa học Giao thông vận tải, Vol.75, No.3, pp.1463-1476.
doi: 10.47869/tcsj.75.3.12.

Received:	28/10/2025
Revised:	08/11/2025
Accepted:	12/11/2025